



OPEN

# Altered internetwork functional connectivity and graph analysis of occipital regions in patients with chronic rhinosinusitis accompanied by olfactory dysfunction

Hongmei Kuang<sup>1,3</sup>, Shunda Hong<sup>1,3</sup>, Yeyuan Chen<sup>1</sup>, Hao Peng<sup>2</sup>, Zihan Li<sup>1</sup>, Yangyang Xie<sup>1</sup>, Wanqing Zhou<sup>1</sup>, Suhong Qin<sup>1</sup>, Jing Ru<sup>1</sup> & Jian Jiang<sup>1</sup>✉

This study assessed whole-brain functional connectivity and network graph theory indices in patients with chronic rhinosinusitis with (CRSwOD) and without (CRSsOD) olfactory dysfunction. We also analyzed correlations between the abnormal network metrics and clinical indices. We acquired resting-state functional magnetic resonance images from 31 patients with CRSsOD, 26 with CRSwOD, and 25 healthy controls (HCs). Functional connectivity was computed and graph theory metrics were evaluated based on the Dosenbach-160 Atlas; relationships between neuroimaging indicators and clinical scales were assessed using Pearson correlation analysis. The results showed that CRSsOD patients had 11 edges with greater strength than HCs, CRSwOD patients had 1 greater edge than HCs, and CRSsOD patients had 5 greater edges than CRSwOD patients. Nodal degree centrality and efficiency in the right posterior occipital region were significantly altered in patients with CRSsOD compared with those in CRSwOD and in HCs. Five and two edges correlated with clinical scales in patients with CRSsOD and CRSwOD, respectively, whereas no correlations in global and nodal indicators were found. These results imply that distinct brain network patterns, particularly in the occipital cortex, could be a valid neuroimaging marker for related diagnosis and prognosis of CRSsOD and CRSwOD patients, and contribute to our better understanding of the central neural mechanisms of CRSwOD, providing new ideas for the clinical management of CRSwOD.

**Keywords** Chronic rhinosinusitis, Olfactory dysfunction, Occipital cortex, Functional connectivity, Graph analysis

Chronic rhinosinusitis (CRS) is a common disease characterized by chronic inflammation of the nasal sinuses, that lasts at least 12 weeks<sup>1</sup>. Olfactory dysfunction (OD) is a relatively common, but an often underestimated problem associated with CRS, presenting in approximately 61–83% of patients<sup>2</sup>. In clinical practice, CRS can be categorized into CRS with OD (CRSwOD) and CRS without OD (CRSsOD) according to the presence or absence of OD in patients<sup>2</sup>. OD can lead to depression, impaired taste, malnutrition, and reduced danger detection which can severely affect quality of life<sup>3,4</sup>.

Normal, healthy nasal membranes transmit aroma information to the brain via the olfactory nerves, enabling odor perception<sup>5</sup>. However, CRS-induced inflammation and congestion can hinder this process and lead to reduced or lost olfactory function<sup>6,7</sup>, however, the exact mechanisms remain unclear<sup>5,8</sup>. Advances in medical imaging and endoscopic modalities have deepened the understanding of CRSwOD, which can be clinically assessed using Lund–Kennedy Endoscopic system (LKES) and Lund–Mackay system (LMS) scores, Sniffin Sticks olfactory tests (Sniffin Sticks threshold, discrimination, and identification, or TDI for short)<sup>9,10</sup>, and the Questionnaire of Olfactory Disorders–Negative Statements (QOD-NS)<sup>10</sup>. Clinical olfactory assessment is time-consuming, laborious, and somewhat subjective. In addition, some patients in clinical practice have normal

<sup>1</sup>Department of Radiology, The First Affiliated Hospital, Nanchang University, Nanchang 330000, Jiangxi, China. <sup>2</sup>Department of Otolaryngology Head and Neck Surgery, The First Affiliated Hospital, Nanchang University, Nanchang 330000, Jiangxi, China. <sup>3</sup>Hongmei Kuang and Shunda Hong contributed equally. ✉email: ndyfy02072@ncu.edu.cn

scores on olfactory function tests but subjectively feel reduced olfactory ability, and deciding whether olfactory ability is truly diminished or if treatment is needed for hyposmia or loss of olfactory function is challenging under such situations<sup>11</sup>. At the same time, there are some patients in clinical practice for whom the treatment of OD is ineffective, and therefore an accurate assessment of their olfactory impairment should be performed before starting treatment, which can help to predict their prognosis and provide appropriate counseling<sup>12</sup>.

Functional magnetic resonance imaging (fMRI) is a noninvasive method that can objectively assess olfactory function in patients and enhance the understanding of OD<sup>13</sup>. The current belief is that OD leads to abnormal activation and structural changes<sup>14–16</sup>. Brain activity in response to odor stimuli in olfactory-related areas such as the pyriform cortex, amygdala, orbitofrontal cortex (OFC), insula, and anterior cingulate cortex is reduced in patients with OD compared with that in healthy persons<sup>17,18</sup>. Furthermore, temporary smell deprivation caused by nasal passage closure modifies activity in brain areas related to processing smells<sup>19</sup>. Previous fMRI studies have largely focused on the olfactory-related regions in patients with CRSwOD<sup>13–20</sup>. However, patients with CRSwOD often have taste, mood, and cognitive dysfunction<sup>14,21,22</sup>. Our previous studies have found higher resting state (rs)-fMRI values for regional homogeneity (ReHo) in cerebellar regions and lower values in the inferior temporal gyrus, precuneus, postcentral, and paracentral gyri of patients with CRSwOD than in those with CRSsOD<sup>15</sup>. Scores for the QOD-NS correlated negatively with ReHo levels in the precuneus and posterior cingulate gyrus of patients with CRSwOD<sup>15</sup>. We have also determined that long-term nasal inflammation influences functional connectivity (FC) in the middle frontal gyrus and OFC, which may serve as a diagnostic imaging marker<sup>16</sup>. The significantly increased amplitude of low-frequency fluctuation (ALFF) in the OFC of patients with CRS positively correlates with Hospital Anxiety and Depression Scale (HADS) scores<sup>14</sup>. Therefore, analyzing abnormal changes in a single olfactory network cannot fully explain the neural mechanisms of CRSwOD.

These previous studies suggest that patients with CRSwOD have abnormal neuronal activity in multiple brain regions other than olfactory-related brain regions; however, the presence of abnormal functional network connections between these brain regions remains unclear. Previously used methods (e.g., ReHo, ALFF, FC) have assessed localized functional activities in the brain, and they have limitations in assessing functional interactions or integration between different brain regions. Graph theory-based functional brain network analysis can analyze complex intra- and inter-network functional connectivity at the whole-brain level. A comparison of these research methods has been presented in tabular form in Supplementary Material S1. Our work advanced the field through the following contributions: (1) The first use of whole-brain network analysis might provide insights into OD due to CRS from different functional networks; (2) Graph analysis of functional connectivity between or within networks might reveal collaborative interactions across the brain, providing new insights into central mechanisms in CRSwOD patients; (3) Graph theory-based functional brain network analysis, we were committed to finding network indicators in specific brain regions to be one of the neuroimaging markers for identifying patients with CRSwOD.

Therefore, the aim of this study was to assess the functional connectivity of whole-brain networks and network graph theory metrics in patients with CRSwOD and CRSsOD, and to analyze the correlation of these imaging metrics with clinical indicators. In addition, this study proposed to look for network metrics in specific brain regions so that CRSwOD patients can be identified among CRS patients, which may serve as a neuroimaging marker to identify CRSwOD patients. Figure 1 shows the workflow of the study.

## Methods

### Participants

We recruited 57 patients, 31 and 26 with CRSsOD and CRSwOD, respectively, and 30 age-matched HCs. The mean ages of the patients with CRSsOD and CRSwOD were  $30.74 \pm 12.79$  and  $42.54 \pm 13.82$  years, respectively.

The inclusion criteria were (1) right-handedness; (2) age 18–55 years; (3) bilateral chronic sinusitis with or without OD clinically diagnosed by two head and neck surgeons according to the European Position Paper on Rhinosinusitis and Nasal Polyps 2020; and (4) ability to cooperate with olfactory and imaging assessments. All recruited patients underwent standard evaluations including endoscopy (assessed as LKES scores), computed tomography of the sinuses (assessed as LMS scores), Patient Health Questionnaire-2 (PHQ-2) scores and the Sniffin Sticks olfactory test (assessed as TDI scores). Participants were also interviewed using the QOD-NS.

Exclusion criteria included patients with (1) dementia or major depression identified using the PHQ-2; (2) preexisting olfactory and gustatory dysfunction, previous head trauma, evidence of allergic rhinitis, or previous chronic sinusitis surgery; neurological diseases or other serious illness; (3) diagnosis of any severe medical condition including hemodynamic instability or significant cardiovascular disease; and (4) contraindications for MRI.

The Institutional Review Board and Medical Research Ethics Committee at the First Affiliated Hospital of Nanchang University approved to this study (ethics approval code: (2022) CDYFYLYK (08–017)), which complied with the ethical principles enshrined in the Declaration of Helsinki (2013 amendment). All recruited patients and healthy volunteers provided written, informed consent to participate in this study and to publish information and images in an online open access publication.

### MRI acquisition

Images were acquired by MRI using a 3-Tesla MR unit (Discovery MR750; GE Healthcare, Milwaukee, WI) equipped with an 8-channel phased array coil. The parameters for rs-fMRI acquisition were as follows: acquisition, 240 time points; flip angle, 90°; matrix,  $64 \times 64$ ; field of view (FOV),  $220 \times 220$  mm; slice thickness, 4 mm; repetition time (TR), 2000 ms; echo time (TE), 30 ms. We also acquired high-resolution anatomical 3D T1-weighted images under the following conditions: TR, 1900 ms; TE, 2.26 ms; flip angle, 9°; matrix,  $240 \times 256$ ; FOV,  $215 \times 230$  mm; slice thickness, 1.0 mm; 176 sagittal slices and T2-weighted images as follows: TR, 4000 ms;

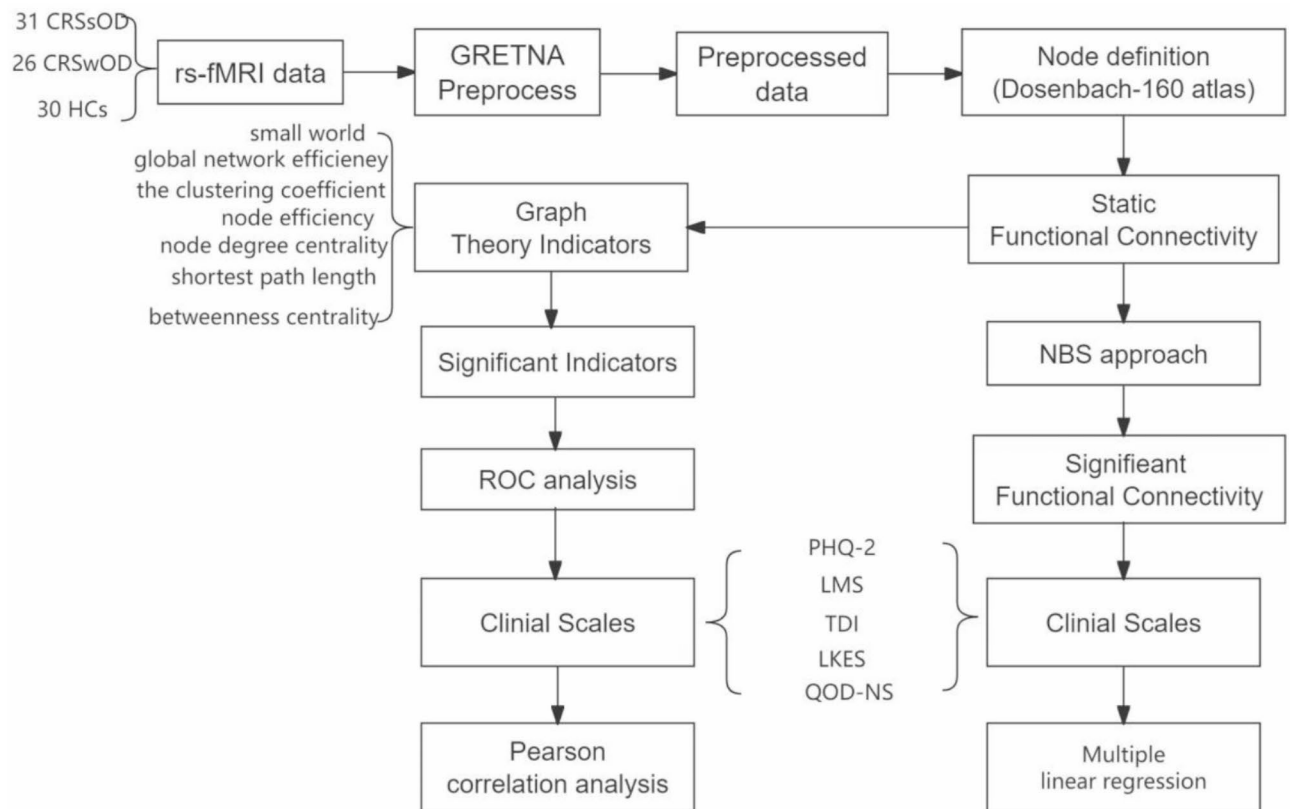


**Fig. 1.** Processing pipeline of rs-fMRI data. *CRSsOD* chronic rhinosinusitis without olfactory dysfunction, *CRSwOD* chronic rhinosinusitis with olfactory dysfunction, *HCS* healthy controls, *LKES* nasal endoscopy Lund–Kennedy score, *LMS* sinus computed tomography (CT) Lund–Mackay score, *NBS* network-based statistic, *ROC* receiver operating characteristic, *rs-fMRI* resting-state functional magnetic resonance imaging, *PHQ-2* Patient Health Questionnaire-2, *QOD-NS* Questionnaire of Olfactory Disorders-Negative Statements, *TDI* threshold, discrimination, and identification in Sniffin Sticks tests.

TE, 113 ms; slices, 19; slice thickness, 5 mm; gap, 1.5 mm; and FOV, 220 × 220 mm. Participants were instructed not to focus on any particular ideas, to keep their eyes closed, and not to doze during the procedure.

### MRI data preprocessing

Data were preprocessed using Statistical Parametric Mapping 12 (SPM12; <http://www.fl.ion.ucl.ac.uk/spm>) in MATLAB 2018b (MathWorks Inc., Natick, MA, USA)<sup>23</sup>. The steps included: conversion from DICOM format; exclusion of the first 10 time points; slice timing and head motion correction; coregistration of high-resolution T1 weighted images to the mean functional image, segmentation into white matter, gray matter, and cerebrospinal fluid using diffeomorphic anatomical registration through exponentiated lie algebra (DARTEL), and resampling to 3 mm isotropic voxels; detrended linear drift; nuisance linear regression (Friston-24 head movement parameters, white matter, cerebrospinal fluid signals); and filtering (0.01–0.08 Hz) to mitigate low-frequency drift and high-frequency physiological noise. We omitted global signal regression to minimize the possibility of functional connection distortion<sup>24,25</sup>. Images were not smoothed to prevent changes in between-group network differences<sup>26</sup>. After excluding those with head motions that exceeded 2 mm in translation and/or 2° in rotation, we analyzed data from 31 to 26 patients with CRSsOD and CRSwOD, respectively, and 25 HCs.

### Definition of nodes

Large-scale functional networks were defined using the Dosenbach-160 atlas. The Dosenbach-160 Atlas is a brain network atlas based on functional connectivity optimization, which shows more robustness than anatomical atlases (e.g., AAL&HOA) in the analysis based on fMRI data, especially in constructing the functional connectivity networks. There are six brain network divisions, frontoparietal network (FPN), occipital network (ON), sensorimotor network (SMN), default mode network (DMN), cinguloopercular network (CON) and cerebellum, which can provide information on brain regions and brain networks see interaction<sup>27</sup>. Theoretically, similar work could be accomplished using the Power-264 Atlas, perhaps with excellent performance. However, while this atlas has a high number of regions, its larger regional divisions may lead to a loss of detail, and in particular may not be as sensitive as the Dosenbach-160 atlas when analyzing smaller or more localized functional connections. We selected this atlas based on meta-analyses of task-related fMRI data. Nodes were

represented using Montreal Neurological Institute (MNI) coordinates and spheres with a 5-mm radius<sup>27</sup> (Supplementary Material S2).

Static functional connectivity and graph analysis

Functional connectivity across regions of interest (ROIs) was determined by converting *r* to *z* values using Fisher’s *Z* transformation and Pearson correlation coefficients (*r*). This produced a 160 × 160 functional connectivity matrix for each participant. Edge strengths and connectivity were calculated using Pearson correlation analysis to calculate the correlation coefficient between two nodes. Global and local graph theory metrics were computed using these matrices, with network sparsity (the ratio of real edges to maximum potential edges) varied in increments of 0.01 from 0.01 to 0.4<sup>25</sup>. Brain and random networks are frequently compared to identify substantial non-randomness in topology. Herein, we set the number of random networks at 100. Small world and global network efficiency were computed as global network measures, and clustering coefficient, node efficiency, node degree centrality, the length of the shortest path, and betweenness centrality were computed as local network measures. The definitions and formulas for these indicators have been described in detail in Supplementary Material S3.

Statistical analysis

Demographic data were statistically analyzed using SPSS 17.0 (SPSS Inc., Chicago, IL., USA). Continuous variables were tested for normality using the Shapiro-Wilk test; continuous variables following a normal distribution were expressed using the mean ± standard deviation, otherwise the median ± quartiles were used. Groups were compared using two-tailed independent sample *t* tests and analysis of variance (ANOVA), and sex proportions were compared using Chi-square tests. All statistical tests were two-tailed and significance was set at *p* < 0.05. To investigate differences in whole-brain functional connectivity among groups, the analysis of covariance (ANCOVA) was performed using *Z*-values in the GRETNA toolbox, post-hoc analysis was performed using the false discovery rate (FDR) correction, and significance thresholds of *p* < 0.05 were applied to the connectivities, with age and sex as covariates. Graph theory metrics were similarly analyzed. Then, the area under curve (AUC) was used to evaluate whether the graph theory metrics could be used to distinguish between CRSwOD patients, CRSsOD patients and HCs. We further explored the correlation between the abnormal imaging data and clinical scales using Pearson correlation analysis. It was then corrected by Bonferroni multiple comparisons. Values with *p* < 0.05 were considered statistically significant.

Results

Clinical and demographic traits

Table 1 summarizes the clinical and demographic information for all subjects. Age and sex did not significantly differ, whereas QOD-NS and TDI scores varied significantly between the groups. Variations in the Patient Health Questionnaire-2 (PHQ-2), LKES, or LMS scores were not discernible. Five healthy volunteers were excluded due to head movement artifacts during MRI data preprocessing.

Modified functional connectivity among HCs and patients with CRSsOD and CRSwOD

To compare the differences in functional connectivity between the three groups, we applied the ANCOVA method. The results showed that CRSsOD patients had 11 edges with greater strength than HCs, CRSwOD patients had 1 greater edge than HCs, and CRSsOD patients had 5 greater edges than CRSwOD patients. Table 2 has shown details of the nodes, affiliated networks, between-group differences, edge data, and statistics. The edges that differ between the three groups have been visualized in Fig. 2A–C.

Group differences in measurements across node networks

To compare between-group differences in node network metrics, we applied the ANCOVA method. The results revealed significant between-group differences in node degree centrality and node efficiency. Specifically, nodal

	CRSsOD (n = 31)	CRSwOD (n = 26)	HC (n = 25)	χ <sup>2</sup> /Z/F value	P value
Demographic data					
Age	30.74 ± 12.79	42.54 ± 13.82	43.68 ± 11.68	2.562	0.201
Sex (male/female)	19/12	19/7	14/11	3.051	0.221
Clinical data					
LKES	6.00 ± 1.57	6.23 ± 2.27	–	0.452	0.653
LMS	13.69 ± 4.97	15.15 ± 5.69	–	1.018	0.313
QOD-NS scores	32.55 ± 11.35	39.69 ± 12.35	–	2.234	0.029
TDI scores	35.97 ± 2.76	11.81 ± 4.85	–	23.010	< 0.001
PHQ-2 scores	1.71 ± 1.19	2.19 ± 1.47	–	1.371	0.176

**Table 1.** Participant information. ANOVA analysis of variance, *LKES* nasal endoscopy, Lund–Kennedy score, *LMS* sinus computed tomography Lund–Mackay score, *PHQ-2* Patient Health Questionnaire-2, *QOD-NS* Questionnaire of Olfactory Disorders–Negative Statements, *TDI* threshold, discrimination, and identification in Sniffin Sticks tests. We compared differences in age, ANOVA, sex, Chi-square test, *LKES*, *LMS*, *QOD-NS*, *TDI*, and *PHQ-2* scores among groups.

	Edges	Internetwork	p-value	T value
CRSwOD > HCs	[7,10]	Default mode, default mode	< 0.001	6.13
CRSsOD > CRSwOD	[77,120]	Cingulo-opercular, sensorimotor	< 0.001	5.55
	[106,116]	Sensorimotor, sensorimotor	< 0.001	5.27
	[106,120]	Sensorimotor, sensorimotor	< 0.001	4.78
	[115,120]	Sensorimotor, sensorimotor	< 0.001	5.49
	[128,136]	Occipital, occipital	< 0.001	5.85
CRSsOD > HCs	[17,133]	Default mode, occipital	< 0.001	1.01
	[47,96]	Frontoparietal, sensorimotor	< 0.001	3.69
	[47,98]	Frontoparietal, sensorimotor	< 0.001	4.09
	[47,108]	Frontoparietal, sensorimotor	< 0.001	4.04
	[46,110]	Frontoparietal, sensorimotor	< 0.001	3.54
	[47,110]	Frontoparietal, sensorimotor	< 0.001	3.82
	[47,111]	Frontoparietal, sensorimotor	< 0.001	3.69
	[66,96]	Cingulo-opercular, sensorimotor	< 0.001	4.36
	[105,110]	Sensorimotor, sensorimotor	< 0.001	3.94
	[110,113]	Sensorimotor, sensorimotor	< 0.001	3.96
	[110,133]	Occipital, sensorimotor	< 0.001	3.70

**Table 2.** Information about edges with between-group differences based on correction ( $p < 0.001$ ; 5000 permutation tests). *CRSsOD* chronic rhinosinusitis without factory dysfunction, *CRSwOD* chronic rhinosinusitis with olfactory dysfunction, *HC* healthy controls.

degree centrality (Fig. 3A, B) and nodal efficiency (Fig. 4A, B) of the right posterior occipital region of the occipital network were significantly altered in patients with CRSsOD compared with those in CRSwOD, and HCs. However, no significant differences were observed between HCs and patients with CRSwOD. Global network measures (small-world and global network efficiency) and other local network measures (clustering coefficient, the length of the shortest path and betweenness centrality) did not significantly differ among the three groups.

Association between abnormal network metrics and clinical scales

In order to explore the relationship between the abnormal network metrics and the clinical scales, we performed a correlation analysis of them. The results of functional connectivity and correlation analyses of patients with CRSsOD revealed significant relationships. The z-scores of edge strength between the left dorsolateral frontal cortex (dFC) and the left mid-insula [47,96] ( $r = -0.409, p = 0.022$ ; Fig. 5A), and between the left dFC and the left parietal cortex [47,98] ( $r = -0.371, p = 0.039$ ; Fig. 5B) significantly correlated with PHQ-2 scores. The z-scores of edge strength between the right and right post occipital cortex [128,136] ( $r = 0.39, p = 0.03$ ) significantly correlated with LMS scores (Fig. 5C). and those of edge strength between the left dFC and the left temporal [47,111] ( $r = 0.39, p = 0.03$ ; Fig. 5D). The z-scores of the left precentral gyrus and the right occipital cortex [110,133] ( $r = 0.46, p = 0.01$ ; Fig. 5E) significantly correlated with TDI scores in patients with CRSwOD. The z-scores of edge strength between the left parietal and the left parietal [106,116] ( $r = -0.40, p = 0.04$ ) significantly correlated with the QOD-NS scores (Fig. 6A). The z-score of edge strength between the right occipital and the right post occipital [128,136] ( $r = -0.40, p = 0.04$ ) significantly correlated with the TDI scores (Fig. 6B). The other 11 and four edges associated with CRSsOD and CRSwOD, respectively, did not significantly correlate with clinical scales. Detailed information was presented as heat maps in Figs. 7 and 8. Relationships between clinical scales and global and nodal graph theory indicators were not discernible in either of the patient groups.

Discussion

We identified 17 significantly different internetwork connections in the frontoparietal (FPN), occipital (ON), sensorimotor (SMN), default mode (DMN), and cinguloopercular (CON) networks among patients with CRSsOD and CRSwOD, as well as HCs. CRSsOD patients showed 11 greater connect edges than HCs' and 1 CRSwODs' greater than HCs'. Meanwhile, 5 connect edges were greater in CRSsOD patients than CRSwODs'. We calculated correlations between differential functional connectivity, PHQ-2 scores, TDI scores, QOD-NS scores, LMS scores and LKES scores. Functional connectivity between the dFC in the FPN and the mid-insula and the parietal cortex in the SMN significantly correlated with PHQ-2 scales in patients with CRSsOD. The prefrontal cortex is responsible for making judgments and executing functions such as processing, and integrating incoming information from multiple connections with various brain regions to decide appropriate emotional and motor responses. The frontal cortex regulates emotions via top-down, higher-order, cognitive executive functions<sup>28</sup>. Emotion regulation may depend on the fronto-limbic network, which includes regions associated with emotions, social behavior, and autonomic nervous system control such as the prefrontal cortex, cingulate gyrus, and amygdala<sup>29</sup>. These areas have a close relationship with the olfactory system and are involved in mood and behavior control<sup>30</sup>. The insula is a motor connection area that plays a key role in body perception and in processing of visceral and somatic sensations<sup>31</sup>. The vagus nerve transmits sensory information upward, passing



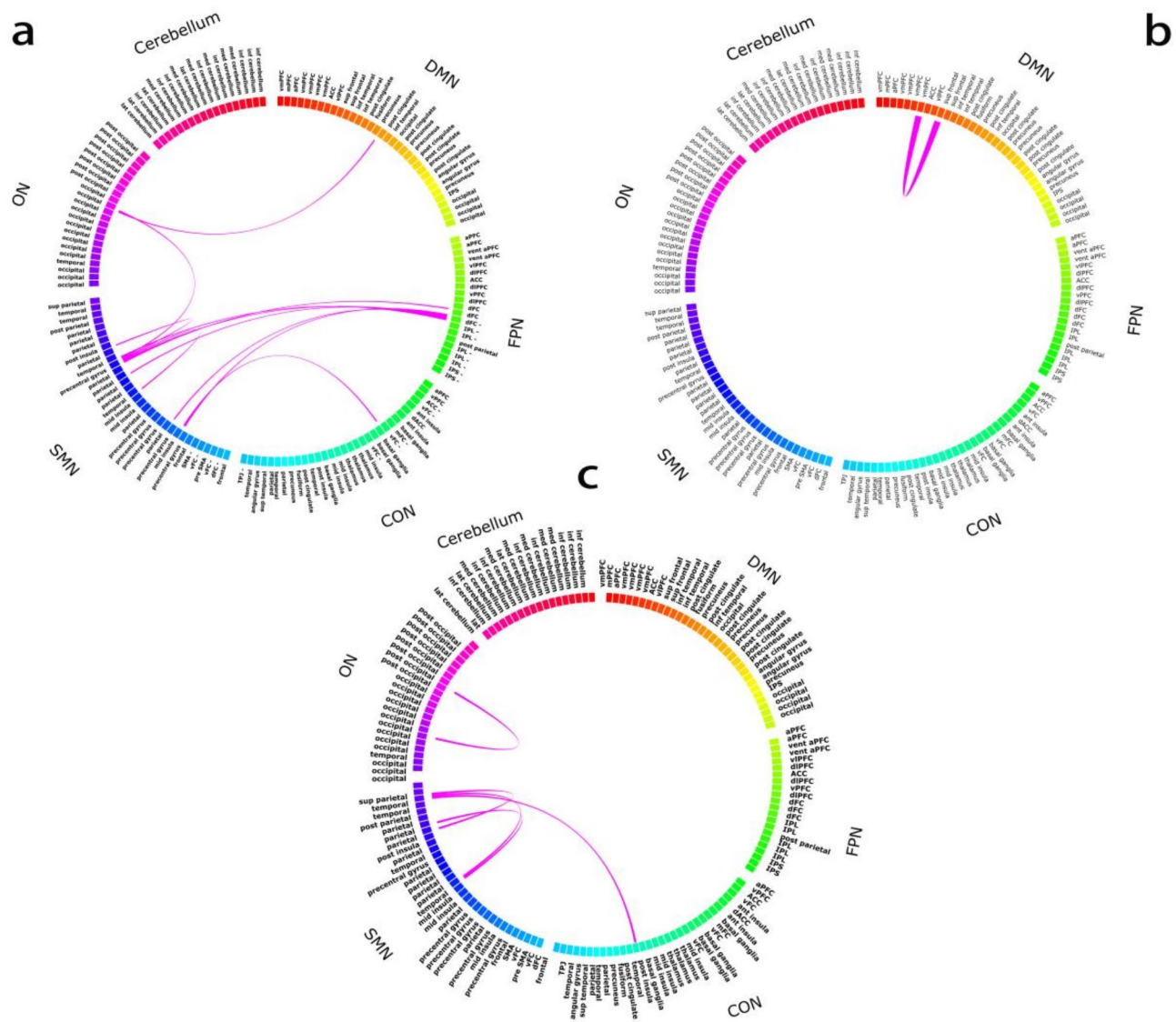


**Fig. 2.** Circle map of functional connectivity between groups determined by ROI–ROI analysis. Distinct brain regions are colored. CON cinguloopercular network, CRSsOD chronic rhinosinusitis without olfactory dysfunction, CRSwOD chronic rhinosinusitis with olfactory dysfunction, DMN default mode network, FPN frontoparietal network, ON occipital network, SMN sensorimotor network, HCs healthy controls, ROI region of interest. (a) CRSsOD > HCs; (b) CRSwOD > HCs; (c) CRSsOD > CRSwOD.

through the autonomic nuclei and thalamus to the insula to integrate sensory information<sup>31</sup>. Therefore, the mid-insula is an important node in the sensory information processing pathway. It is also part of the secondary olfactory network and participates in postoperative reconstruction of the function and structure of the central olfactory network in patients with chronic sinusitis<sup>32</sup>. Like the mid-insula, the parietal cortex is also related to physical sensations; it receives tactile signals under external stimulation and generates corresponding motor responses<sup>33</sup>. The present study found that the functional connectivity of the dFC and the mid-insula and parietal cortex correlated significantly and negatively with the PHQ-2 scores in patients with CRSsOD. These suggest that patients with CRSsOD have altered functional connectivity in emotion regulation and sensorimotor related brain regions, and that this alteration of brain functional connectivity may further exacerbate the depressive state of CRSsOD patients. The dFC is considered an important region for the cognitive behavioral treatment of depression<sup>34</sup>. Significantly reduced functional connectivity between the dFC and the anterior cingulate cortex normalizes in patients after treatment for depression<sup>35</sup>. Task-based fMRI studies showed that the abnormalities in dFC activity were linked to emotional tasks in patients with major depressive disorder<sup>36,37</sup>. These findings suggest that the dFC is associated with emotion regulation and cognitive function. It is well known that comorbid depression significantly increases the disease burden in 20–30% of patients with CRS<sup>38,39</sup>. The severity of depression notably improves in patients with CRS after endoscopic nasal surgery<sup>40</sup>. Our study participants did not have comorbid depression. Thus, given the capacity of the brain to adapt and compensate, our results might reflect early or subclinical functional changes in the brain. If so, behavioral responses might be more sensitive

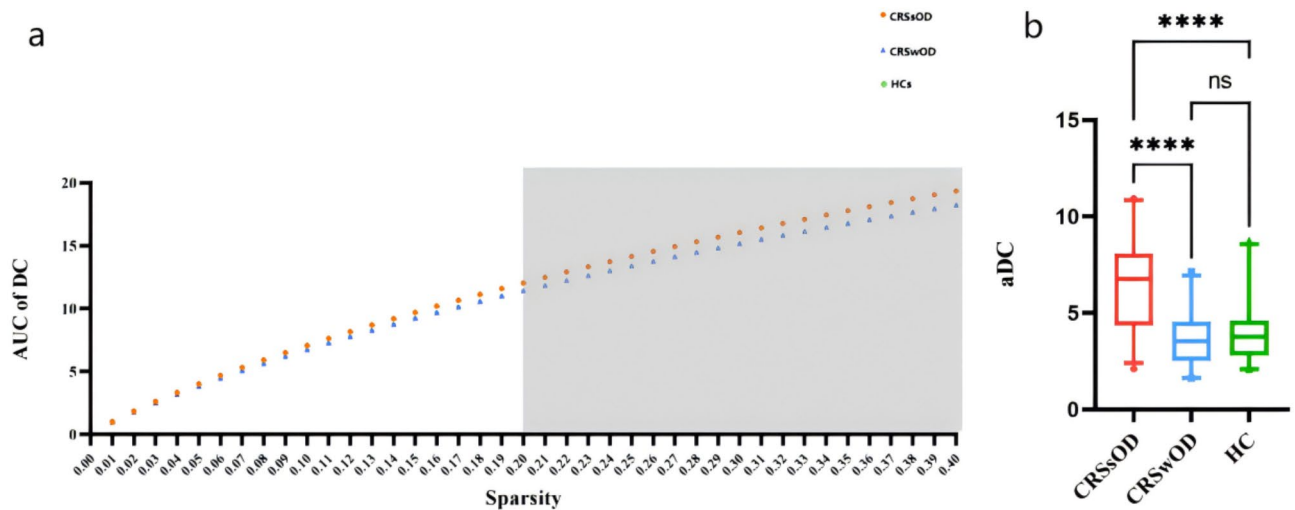


**Fig. 3.** (a) Average curves of nodal degree centrality for right posterior occipital region among 40 network sparsity values. Y-axis represents nodal degree of centrality for each sparsity level in one group. Gray shading indicates areas of sparsity that significantly differed. (b) Nodal degree centrality of 40 network sparsity values in right posterior occipital region among CRSsOD, CRSwOD, and HCs determined using AUC. Each dot represents AUC for sparsity in one participant. No differences were significant between patients with CRSwOD and HCs. AUC area under ROC curve, CRSsOD chronic rhinosinusitis without olfactory dysfunction, CRSwOD chronic rhinosinusitis with olfactory dysfunction, HCs healthy controls.

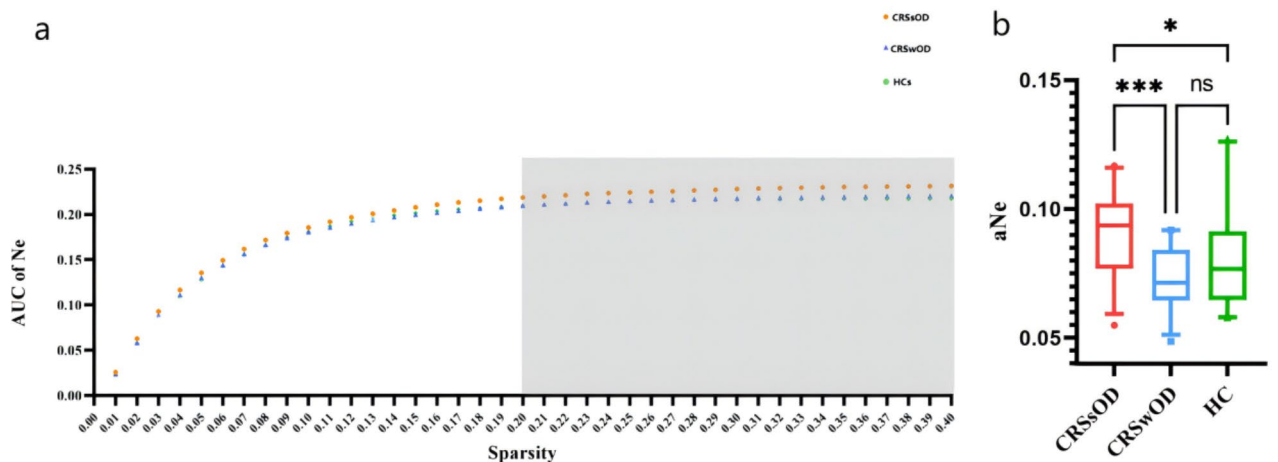


**Fig. 4.** (a) Average curves of node efficiency for right posterior occipital region among 40 network sparsity values. Y-axis, node efficiency of each sparsity level in one group. Gray shading indicates significant differences. (b) Node efficiency in right posterior occipital region among 40 network sparsity values in CRSsOD, CRSwOD, and HCs groups determined by AUCs. Each dot represents AUC for all sparsity in one participant. None of three groups significantly differed. AUC area under ROC curve, CRSsOD chronic rhinosinusitis without olfactory dysfunction, CRSwOD chronic rhinosinusitis with olfactory dysfunction, HCs healthy controls, ROC receiver operating characteristic.

than these responses, indicating that changes in emotional regulatory and sensorimotor-related brain regions occur before the onset of depression symptoms in patients with CRSsOD. This might provide early imaging evidence of comorbid depression in CRS. This study also found that the functional connectivity of dFC and temporal in patients with CRSsOD was significantly positively correlated with TDI scores. The main functional areas of temporal include the olfactory center (uncus and anterior hippocampus), the auditory center (middle superior temporal gyrus and transverse temporal gyrus), and the sensory language center (posterior superior temporal gyrus). The increased functional connectivity of dFC and temporal may activate the olfactory center, thereby compensating for the olfactory abilities of patients with CRSsOD. The inferior parietal cortex is associated with memory and semantic processing, and if memory is used to initiate a task, the short-term memory area of the prefrontal cortex becomes active<sup>41</sup>, such as connected areas in the posterior parietal cortex<sup>42</sup>. Initiating a task

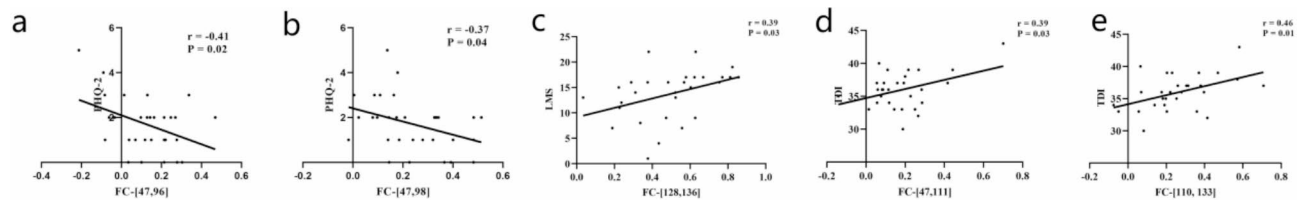


**Fig. 5.** Correlation analysis of brain regions associated with FC abnormalities and clinical scales in patients with CRSsOD. **(a)** Correlation with PHQ-2 scores between left dorsolateral frontal cortex (dFC) and left mid-insula [47,96]. **(b)** Correlations with PHQ-2 scores between left dorsolateral frontal (dFC) and left parietal cortex [47,98]. **(c)** Correlations with LMS scores between right occipital and right post occipital regions [128,136] in patients with CRSsOD. **(d)** Correlation analysis of TDI scores between left dFC and left temporal [47,111] cortices in patients with CRSsOD. **(e)** Correlations with TDI scores between left precentral gyrus and right occipital region [110,133]. *CRSsOD* chronic rhinosinusitis without olfactory dysfunction, *CT* computed tomography, *dFC* dorsolateral frontal cortex, *FC* functional connectivity, *LMS* sinus computed tomography Lund–Mackay score, *PHQ-2* Patient Health Questionnaire-2, *TDI* threshold, discrimination, and identification in Sniffin Sticks tests.

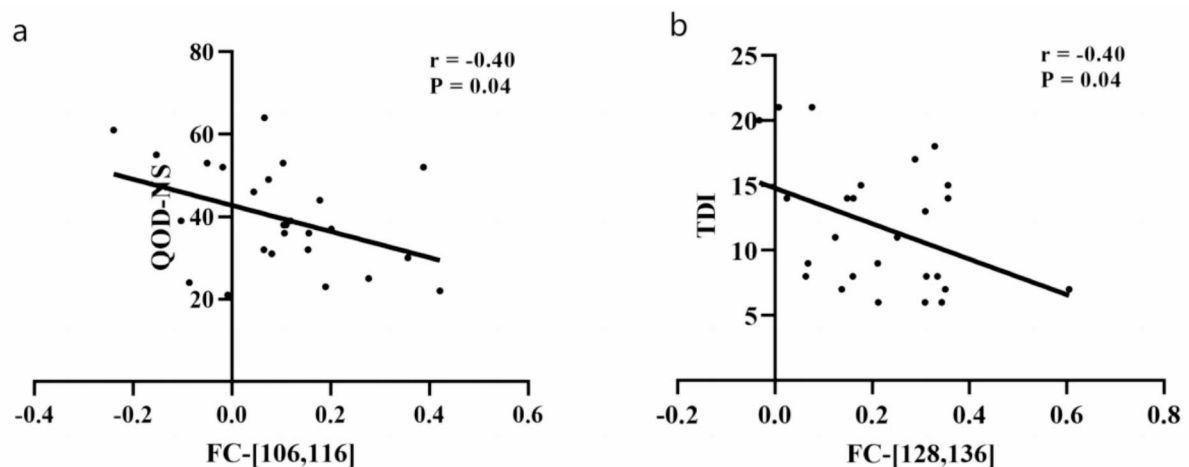


**Fig. 6.** Correlation analysis of brain regions associated with FC abnormalities and clinical scales in patients with CRSwOD. **(a)** Correlations between QOD-NS scores in left parietal cortices [106,116] and **(b)** between TDI scores in right occipital and right post-occipital regions [128,136] in patients. *CRSwOD* chronic rhinosinusitis with olfactory dysfunction, *FC* functional connectivity, *QOD-NS* Questionnaire of Olfactory Disorders-Negative Statements, *TDI* threshold, discrimination, and identification in Sniffin Sticks tests.

using memory is crucial to understanding the dFC and its connections with parietal regions<sup>41</sup>. The abnormal functional connectivity between the dFC and parietal cortex in the present study might be attributed to long-term, negative affective memories. In patients with CRSwOD, we found decreased functional connectivity between parietal regions in SMN, which was significantly negatively correlated with QOD-NS scores. This suggests that the functional connectivity between parietal regions in patients with CRSwOD may be impaired, likely due to long-term stimulation of negative emotional memories, leading to a decompensation in the parietal lobe's ability to process memory. Consequently, patients with CRSwOD experience a poorer quality of life due to olfactory dysfunction. We also found that in patients with CRSsOD, the functional connectivity between the occipital and post-occipital in ON was increased and significantly positively correlated with LMS scores. Meanwhile, in patients with CRSwOD, the functional connectivity between the occipital and post-occipital in ON was decreased and significantly negatively correlated with TDI scores. The occipital lobe is the primary brain region for processing and regulating visual information, and it also receives and processes non-visual information, including olfactory stimuli<sup>43</sup>. Brain activation studies performed with fMRI scans have shown that several regions of the occipital cortex were recruited during active conditions of olfactory processing in humans affected by early blindness<sup>43</sup>. Other studies have shown that there is activation in the brain's visual areas during the processing of olfactory tasks<sup>44</sup>. The activation foci in the occipital cortex of sighted individuals would be caused by visual imagery of objects induced by odor perception<sup>45</sup>. Meanwhile, visual brain areas might also be involved in hedonic judgments and semantic processing of odors<sup>46</sup>. These studies indicate that the occipital lobe plays a certain role in olfactory processing. This is consistent with our observations that the increased functional connectivity between the occipital and post-occipital in ON of CRSsOD patients is positively correlated with



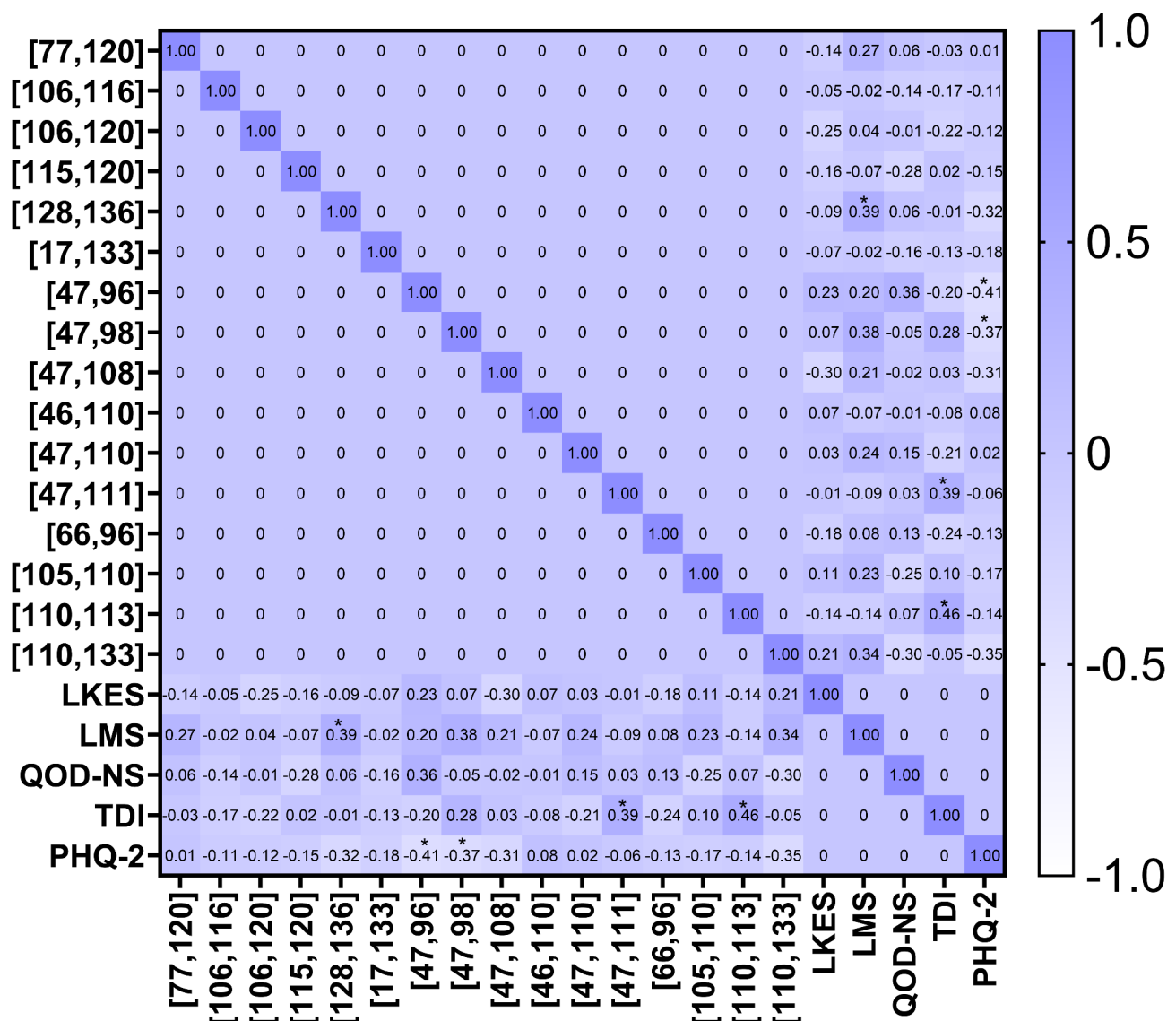


**Fig. 7.** Heatmap of the correlation coefficients between each brain region associated with FC ([77,120], [106,116], [106,120], [115,120], [128,136], [17,133], [47,96], [47,98], [47,108], [46,110], [47,110], [47,111], [66,96], [105,110], [110,113], [110,133]) and each scale (LKES, LMS, QOD-NS, TDI, and PHQ-2) in the CRSsOD group. Purple indicates positive correlation and white indicates negative correlation; the darker the color, the stronger the correlation. A diagonal line set to 1.00 represents a full positive correlation between the variable and itself, and a display of 0 indicates that no correlation was analyzed between these two variables. Correlation coefficients with an asterisk (\*) indicate statistical significance ( $p < 0.05$ ). *FC* functional connectivity, *LKES* nasal endoscopy Lund–Kennedy score, *LMS* sinus computed tomography (CT) Lund–Mackay score, *NBS* network-based statistic, *ROC* receiver operating characteristic, *rs-fMRI* resting-state functional magnetic resonance imaging, *PHQ-2* Patient Health Questionnaire-2, *QOD-NS* Questionnaire of Olfactory Disorders-Negative Statements, *TDI* threshold, discrimination, and identification in Sniffin Sticks tests.

the severity of sinusitis, suggesting that the worsening of sinusitis further activates the occipital lobe in olfactory processing, thereby helping CRSsOD patients maintain better olfactory function. However, in patients with CRSwOD, the decreased functional connectivity between the occipital and post-occipital in ON suggests that the function of the occipital lobe in olfactory processing may be impaired, further exacerbating the olfactory dysfunction in CRSwOD patients. Therefore, the occipital lobe is likely to be a neuroimaging target that mediates olfactory dysfunction in patients with chronic rhinosinusitis.

The FPN plays a core role in regulating cognition through extensive connections with other brain regions<sup>47</sup>. The FPN is an important control center for higher-level neural processing and its activity increases during complex cognitive tasks<sup>47,48</sup>. Dysfunction within this network might lead to psychopathology, including schizophrenia, anxiety, and major depression<sup>48,49</sup>. Notable functional changes in the FPN of patients with CRS but no discernible clinical mental illness have suggested a relationship between the cognitive effects of CRS and

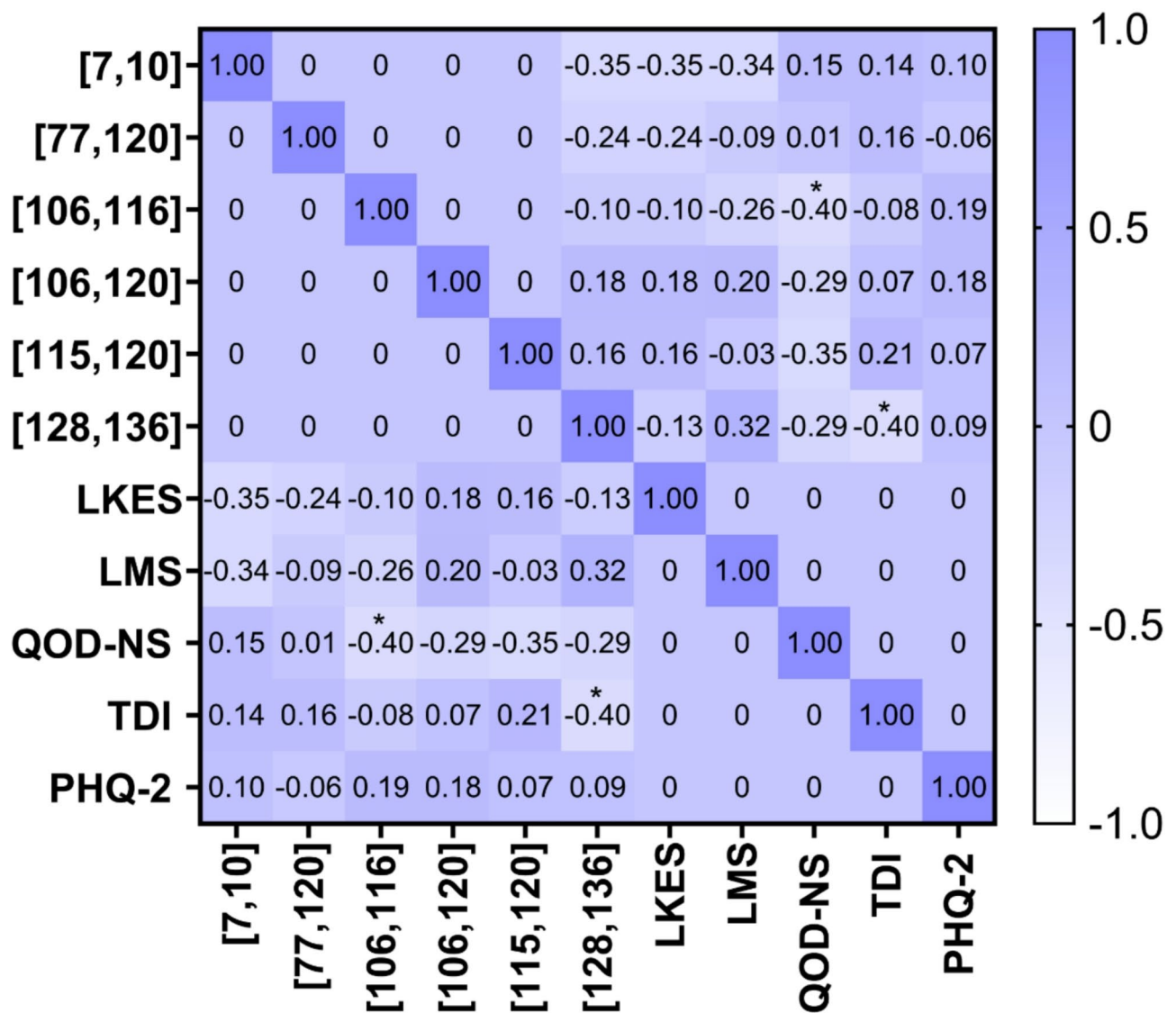


**Fig. 8.** Heatmap of the correlation coefficients between each brain region associated with FC ([7,10], [77,120], [106,116], [106,120], [115,120], [128,136]) and each scale (LKES, LMS, QOD-NS, TDI, and PHQ-2) in the CRSwOD group. Purple indicates positive correlation, white indicates negative correlation, and the darker the color, the stronger the correlation. A diagonal line set to 1.00 represents a full positive correlation between the variable and itself, and a display of 0 indicates that no correlation was analyzed between these two variables. Correlation coefficients with an asterisk (\*) indicate statistical significance ( $p < 0.05$ ). *FC* functional connectivity, *LKES* nasal endoscopy Lund–Kennedy score, *LMS* sinus computed tomography (CT) Lund–Mackay score, *NBS* network-based statistic, *ROC* receiver operating characteristic, *rs-fMRI* resting-state functional magnetic resonance imaging, *PHQ-2* Patient Health Questionnaire-2, *QOD-NS* Questionnaire of Olfactory Disorders-Negative Statements, *TDI* threshold, discrimination, and identification in Sniffin Sticks tests.

depression<sup>50</sup>. The SMN might contribute to general cognitive function in addition to its specialized handling of sensory stimuli and motor responses<sup>51,52</sup>. The functional network connections of key nodes of the SMN are associated with the cognitive control of task switching<sup>53</sup>. We found increased connectivity between the SMN and FPN in patients with CRSsOD compared with HCs. The FPN includes the prefrontal cortex, which is closely connected to the olfactory system. Therefore, we believe that enhanced connectivity between the SMN and FPN in patients with CRSsOD supports the maintenance of olfactory and cognitive functions. We also found lower connectivity within the SMN of patients with CRSsOD than in those with CRSwOD. Further correlation analysis revealed that functional connectivity among the sensorimotor cortices correlated significantly and negatively with the QOD-NS scores of patients with CRSwOD. This might have been due to a loss of olfactory function, which would lead to damaged functional connectivity in the SMN and affect the cognitive control of task switching and consequently worsen the olfactory experience. Functional connectivity was enhanced within the DMN of patients with CRSwOD but not in HCs. When the mind is not focused on a particular activity,

the DMN is the most active network and represents functions such as memory, social interaction, and future planning<sup>54</sup>. The increase in functional connectivity within the DMN in patients with CRSwOD might explain excessive self-focus, possibly resulting from negative emotions that accompany the loss of olfactory function.

Network graph theory metrics revealed significantly increased nodal degree and efficiency in the right post occipital gyrus in the occipital network of patients with CRSsOD than in those CRSwOD and in HCs. Node degree reflects the information communication capability of a node brain region within a functional network<sup>55</sup>. Node efficiency reflects the efficiency of parallel information transmission of a node brain region within a functional network<sup>55</sup>. The occipital gyrus is not considered a traditional olfactory region. From an anatomic perspective, the occipital lobe has extensive fiber connections with the temporal and frontal lobes, which include the secondary olfactory centers responsible for smell memory and perception. Therefore, we tested the hypothesis that the occipital lobe is involved in processing olfactory information. The volume of gray matter is decreased in the occipital lobes of patients with congenital Parkinson's disease and anosmia<sup>56</sup>. Activation of the occipital cortex after exposure to a smell stimulus is widespread in volunteers with normal olfaction<sup>57</sup>. A comparison of congenitally blind patients with healthy volunteers revealed that smell stimuli are preferentially directed to the occipital lobe in the absence of visual input, suggesting its involvement in smell processing<sup>58</sup>. Smell scores and occipital gray matter volume positively correlate in patients with trauma-induced anosmia<sup>59</sup>. Overall, the above findings indicate an association between the occipital cortex and olfaction, and that activation of the occipital cortex plays a positive role in processing olfactory information. The present findings concur with these results. The increased nodal degree and efficiency of the occipital region in patients with CRSsOD might be the basis of maintained olfaction. Meanwhile, the area under curve (AUC) of the nodal degree and nodal efficiency of the right posterior occipital shows that it can be used to distinguish between CRSsOD and CRSwOD. Thus, the occipital may be an important neuroimaging marker for diagnosing and predicting CRSsOD and CRSwOD.

### Limitations

Our study has several limitations. First, although the CRSwOD and CRSsOD patients we recruited had not undergone surgical treatment before the scan and had not taken any medication within 24 h, we could not control whether they had taken medication at an earlier time. Although this situation has almost negligible impact on our results. Second, we did not explore the correlation between the patients' disease duration and neuroimaging data because most patients had a long disease duration, making it difficult for them to provide an accurate duration. Third, we initially performed a cross-sectional study of neuroimages acquired from patients and healthy persons with data from only one rs-fMRI assessment. Longitudinal studies are required to supplement our results and enhance the understanding of CRSwOD and CRSsOD, as well as to validate and enhance our findings. Fourth, analyses of variations in additional neuroimaging indicators were constrained by the small sample size of patients and healthy volunteers. We did not analyze olfactory transduction pathways in patients with CRSwOD. We were unable to accumulate enough clinical data to substantiate possible anomalies in a few network functions. We intend to address these issues in the future, such as increasing the sample size, following up with dynamic network study analysis and modularity, conducting further longitudinal studies, and performing task-based fMRI studies.

### Conclusion

We evaluated network patterns in patients with CRSsOD and CRSwOD via a whole-brain network approach. Node degree centrality and efficiency were lower in patients with CRSwOD than in those with CRSsOD, and lower functional connectivity between the occipital cortex in the ON was associated with TDI scores. Node degree centrality and efficiency might distinguish between patients with CRSsOD and CRSwOD. Differential brain network patterns might serve as valid neuroimaging markers for the diagnosis and prognosis of patients with CRSsOD and CRSwOD, and contribute to our better understanding of the central mechanisms of CRSwOD, providing new ideas for the clinical management of CRSwOD.

### Data availability

Relevant data supporting this study were obtained from the First Affiliated Hospital of Nanchang University, but these data were used under license for the current study and are therefore not publicly available. However, the data can be obtained from the corresponding author upon reasonable request and permission from the First Affiliated Hospital of Nanchang University.

Received: 27 August 2024; Accepted: 25 March 2025

Published online: 31 March 2025

### References

1. Sundaresan, A. S. et al. Occupational and environmental risk factors for chronic rhinosinusitis: A systematic review. *Int. Forum Allergy Rhinol.* <https://doi.org/10.1002/alar.21573> (2015).
2. Ahmed, O. G. & Rowan, N. R. Olfactory dysfunction and chronic rhinosinusitis. *Immunol. Allergy Clin. North Am.* <https://doi.org/10.1016/j.jiac.2019.12.013> (2020).
3. Croy, L., Nordin, S. & Hummel, T. Olfactory disorders and quality of life—An updated review. *Chem. Senses.* <https://doi.org/10.1093/chemse/bjt072> (2014).
4. Schlosser, R. J. et al. Association of olfactory dysfunction in chronic rhinosinusitis with economic productivity and medication usage. *Int. Forum Allergy Rhinol.* <https://doi.org/10.1002/alar.21841> (2017).
5. Bothwell, A. R., Resnick, S. M., Ferrucci, L. & Tian, Q. Associations of olfactory function with brain structural and functional outcomes. A systematic review. *Ageing Res. Rev.* <https://doi.org/10.1016/j.arr.2023.102095> (2023).
6. Hauser, L. J., Chandra, R. K., Li, P. & Turner, J. H. Role of tissue eosinophils in chronic rhinosinusitis-associated olfactory loss. *Int. Forum Allergy Rhinol.* <https://doi.org/10.1002/alar.21994> (2017).

7. Zhang, L. et al. Correlation of tissue eosinophil count and chemosensory functions in patients with chronic rhinosinusitis with nasal polyps after endoscopic sinus surgery. *Eur. Arch. Oto-Rhino-Laryngol.* <https://doi.org/10.1007/s00405-019-05413-9> (2019).
8. Ahmed, O. G. & Rowan, N. R. Olfactory dysfunction and chronic rhinosinusitis. *Immunol. Allergy Clin. North Am.* <https://doi.org/10.1016/j.iac.2019.12.013> (2020).
9. Hummel, T., Kobal, G., Gudziol, H. & Mackay-Sim, A. Normative data for the sniffin' sticks including tests of odor identification, odor discrimination, and olfactory thresholds: An upgrade based on a group of more than 3,000 subjects. *Eur. Arch. Oto-Rhino-Laryngol.* <https://doi.org/10.1007/s00405-006-0173-0> (2007).
10. Mattos, J. L., Schlosser, R. J., Mace, J. C., Smith, T. L. & Soler, Z. M. Establishing the minimal clinically important difference for the questionnaire of olfactory disorders. *Int. Forum Allergy Rhinol.* <https://doi.org/10.1002/alf.22135> (2018).
11. Chung, M. S., Choi, W. R., Jeong, H. Y., Lee, J. H. & Kim, J. H. MR imaging-based evaluations of olfactory bulb atrophy in patients with olfactory dysfunction. *Am. J. Neuroradiol.* <https://doi.org/10.3174/ajnr.A5491> (2018).
12. Rombaux, P., Huart, C., Deggouj, N., Duprez, T. & Hummel, T. Prognostic value of olfactory bulb volume measurement for recovery in postinfectious and posttraumatic olfactory loss. *Otolaryngol. Head Neck Surg.* <https://doi.org/10.1177/0194599812459704> (2012).
13. Han, P., Zang, Y., Akshita, J. & Hummel, T. Magnetic resonance imaging of human olfactory dysfunction. *Brain Topogr.* <https://doi.org/10.1007/s10548-019-00729-5> (2019).
14. Lin, S. et al. Intrinsic brain abnormalities in chronic rhinosinusitis associated with mood and cognitive function. *Front. Neurosci.* <https://doi.org/10.3389/fnins.2023.1131114> (2023).
15. Zhang, Z. et al. Regional homogeneity alterations of resting-state functional magnetic resonance imaging of chronic rhinosinusitis with olfactory dysfunction. *Front. Neurosci.* <https://doi.org/10.3389/fnins.2023.1146259> (2023).
16. Ma, Y. et al. Abnormal functional connectivity of the core olfactory network in patients with chronic rhinosinusitis accompanied by olfactory dysfunction. *Front. Neurol.* <https://doi.org/10.3389/fneur.2023.1295556> (2023).
17. Han, P. et al. Impaired brain response to odors in patients with varied severity of olfactory loss after traumatic brain injury. *J. Neurol.* <https://doi.org/10.1007/s00415-018-9003-8> (2018).
18. Pellegrino, R. et al. Olfactory function in patients with hyposmia compared to healthy subjects—An fMRI study. *Rhinology.* <https://doi.org/10.4193/Rhino16.098> (2016).
19. Wei, H. L. et al. Impaired intrinsic functional connectivity between the thalamus and visual cortex in migraine without aura. *J. Headache Pain.* <https://doi.org/10.1186/s10194-019-1065-1> (2019).
20. Whitcroft, K. L. et al. Structural plasticity of the primary and secondary olfactory cortices: Increased gray matter volume following surgical treatment for chronic rhinosinusitis. *Neuroscience.* <https://doi.org/10.1016/j.neuroscience.2018.10.011> (2018).
21. Nordin, S., Blomqvist, E. H., Olsson, P., Stjerne, P. & Ehnhage, A. Effects of smell loss on daily life and adopted coping strategies in patients with nasal polyposis with asthma. *Acta Oto-Laryngol.* <https://doi.org/10.3109/00016489.2010.539625> (2011).
22. Rombaux, P., Huart, C., Levie, P., Cingi, C. & Hummel, T. Olfaction in chronic rhinosinusitis. *Curr. Allergy Asthma Rep.* <https://doi.org/10.1007/s11882-016-0617-6> (2016).
23. Wang, J. et al. GREYNET: A graph theoretical network analysis toolbox for imaging connectomics. *Front. Hum. Neurosci.* <https://doi.org/10.3389/fnhum.2015.00386> (2015).
24. Murphy, K. & Fox, M. D. Towards a consensus regarding global signal regression for resting state functional connectivity MRI. *Neuroimage.* <https://doi.org/10.1016/j.neuroimage.2016.11.052> (2017).
25. Garrison, K. A., Scheinost, D., Finn, E. S., Shen, X. & Constable, R. T. The (in)stability of functional brain network measures across thresholds. *Neuroimage.* <https://doi.org/10.1016/j.neuroimage.2015.05.046> (2015).
26. Triana, A. M., Glerean, E., Saramaki, J. & Korhonen, O. Effects of Spatial smoothing on group-level differences in functional brain networks. *Netw. Neurosci.* [https://doi.org/10.1162/netn\\_a\\_00132](https://doi.org/10.1162/netn_a_00132) (2020).
27. Dosenbach, N. U. et al. Prediction of individual brain maturity using fMRI. *Science.* <https://doi.org/10.1126/science.1194144> (2010).
28. Seminowicz, D. A. et al. Limbic-frontal circuitry in major depression: A path modeling meta-analysis. *Neuroimage.* <https://doi.org/10.1016/j.neuroimage.2004.01.015> (2004).
29. Catani, M., Dell'Acqua, F., De Schotten, M. & Thiebaut A revised limbic system model for memory, emotion and behaviour. *Neurosci. Biobehav. Rev.* <https://doi.org/10.1016/j.neubiorev.2013.07.001> (2013).
30. McLachlan, R. S. A brief review of the anatomy and physiology of the limbic system. *Can. J. Neurol. Sci.* **36**, S84–S87 (2009).
31. Molnar-Szakacs, I. & Uddin, L. Q. Anterior Insula as a gatekeeper of executive control. *Neurosci. Biobehav. Rev.* <https://doi.org/10.1016/j.neubiorev.2022.104736> (2022).
32. Whitcroft, K. L., Noltus, J., Andrews, P. & Hummel, T. Sinonasal surgery alters brain structure and function: Neuroanatomical correlates of olfactory dysfunction. *J. Neurosci. Res.* <https://doi.org/10.1002/jnr.24897> (2021).
33. Rolls, E. T., Deco, G., Huang, C. C. & Feng, J. The human posterior parietal cortex: Effective connectome, and its relation to function. *Cereb. Cortex* <https://doi.org/10.1093/cercor/bhac266> (2023).
34. Wu, Z. et al. Abnormal functional connectivity of Habenula in untreated patients with first-episode major depressive disorder. *Psychiatry Res.* <https://doi.org/10.1016/j.psychres.2020.112837> (2020).
35. Zhou, W. et al. Differential patterns of dynamic functional connectivity variability in major depressive disorder treated with cognitive behavioral therapy. *J. Affect. Disord.* <https://doi.org/10.1016/j.jad.2021.05.017> (2021).
36. Zheng, M. et al. Dorsolateral prefrontal activation in depressed young adults with and without suicidal ideation during an emotional autobiographical memory task: A fNIRS study. *J. Affect. Disord.* <https://doi.org/10.1016/j.jad.2023.01.115> (2023).
37. Hsu, D. T., Langenecker, S. A., Kennedy, S. E., Zubieta, J. K. & Heitzeg, M. M. fMRI BOLD responses to negative stimuli in the prefrontal cortex are dependent on levels of recent negative life stress in major depressive disorder. *Psychiatry Res.* <https://doi.org/10.1016/j.pscychres.2009.12.002> (2010).
38. Alt, J. A., Mace, J. C., Smith, T. L. & Soler, Z. M. Endoscopic sinus surgery improves cognitive dysfunction in patients with chronic rhinosinusitis. *Int. Forum Allergy Rhinol.* <https://doi.org/10.1002/alf.21820> (2016).
39. Wasan, A., Fernandez, E., Jamison, R. N. & Bhattacharyya, N. Association of anxiety and depression with reported disease severity in patients undergoing evaluation for chronic rhinosinusitis. *Ann. Otol. Rhinol. Laryngol.* <https://doi.org/10.1177/000348940711600703> (2007).
40. Litvack, J. R., Mace, J. & Smith, T. L. Role of depression in outcomes of endoscopic sinus surgery. *Otolaryngol. Head Neck Surg.* <https://doi.org/10.1177/0194599810391625> (2011).
41. Passingham, R. E. & Lau, H. Do we understand the prefrontal cortex? *Brain Struct. Funct.* <https://doi.org/10.1007/s00429-022-02587-7> (2023).
42. Papagno, C. Memory deficits. *Handb. Clin. Neurol.* <https://doi.org/10.1016/B978-0-444-63622-5.00019-X> (2018).
43. Araneda, R., Renier, L. A., Rombaux, P. & Cuevas, I. and A. G. De Volder. Cortical plasticity and olfactory function in early blindness. *Front. Syst. Neurosci.* <https://doi.org/10.3389/fnsys.2016.00075> (2016).
44. Renier, L. et al. and A. G. De Volder. Right occipital cortex activation correlates with superior odor processing performance in the early blind. *PLoS One.* <https://doi.org/10.1371/journal.pone.0071907> (2013).
45. Royet, J. P. et al. Functional neuroanatomy of different olfactory judgments. *Neuroimage* <https://doi.org/10.1006/nimg.2000.0704> (2001).
46. Plailly, J. et al. Involvement of right piriform cortex in olfactory familiarity judgments. *Neuroimage.* <https://doi.org/10.1016/j.neuroimage.2004.10.028> (2005).



47. Marek, S. & Dosenbach, N. U. F. Control networks of the frontal lobes. *Handb. Clin. Neurol.* <https://doi.org/10.1016/B978-0-12-804281-6.00018-5> (2019).
48. Scolari, M., Seidl-Rathkopf, K. N. & Kastner, S. Functions of the human frontoparietal attention network: Evidence from neuroimaging. *Curr. Opin. Behav. Sci.* <https://doi.org/10.1016/j.cobeha.2014.08.003> (2015).
49. Cole, M. W., Repovs, G. & Anticevic, A. The frontoparietal control system: A central role in mental health. *Neuroscientist* <https://doi.org/10.1177/1073858414525995> (2014).
50. Jafari, A. et al. Association of sinonasal inflammation with functional brain connectivity. *JAMA Otolaryngol. Head Neck Surg.* <https://doi.org/10.1001/jamaoto.2021.0204> (2021).
51. Chenji, S. et al. Investigating default mode and sensorimotor network connectivity in amyotrophic lateral sclerosis. *PLoS One*. <https://doi.org/10.1371/journal.pone.0157443> (2016).
52. Bagarinao, E. et al. Reorganization of brain networks and its association with general cognitive performance over the adult lifespan. *Sci. Rep.* <https://doi.org/10.1038/s41598-019-47922-x> (2019).
53. Mofrad, F., Tabassi, A., Jahn & Schiller, N. O. Dual function of primary somatosensory cortex in cognitive control of language: Evidence from resting state fMRI. *Neuroscience*. <https://doi.org/10.1016/j.neuroscience.2020.08.032> (2020).
54. Buckner, R. L., Andrews-Hanna, J. R. & Schacter, D. L. The brain's default network: Anatomy, function, and relevance to disease. *Ann. N Y Acad. Sci.* <https://doi.org/10.1196/annals.1440.011> (2008).
55. Latora, V. & Marchiori, M. Efficient behavior of small-world networks. *Phys. Rev. Lett.* <https://doi.org/10.1103/PhysRevLett.87.198701> (2001).
56. Chen, S. et al. Imaging of olfactory bulb and Gray matter volumes in brain areas associated with olfactory function in patients with Parkinson's disease and multiple system atrophy. *Eur. J. Radiol.* <https://doi.org/10.1016/j.ejrad.2013.11.024> (2014).
57. Ciorba, A. et al. Functional magnetic resonance imaging in the olfactory perception of the same stimuli. *Life-Basel*. <https://doi.org/10.3390/life11010011> (2020).
58. Kupers, R. et al. Neural correlates of olfactory processing in congenital blindness. *Neuropsychologia*. <https://doi.org/10.1016/j.neuropsychologia.2011.03.033> (2011).
59. Gao, X. et al. Patterns of gray and white matter volume alterations in patients with post-traumatic anosmia: A voxel-based morphometry study. *Front. Neurol.* <https://doi.org/10.3389/fneur.2022.690760> (2022).

## Acknowledgements

We thank all subjects for their participation in scanning and all medical staff of the department of Radiology and Otolaryngology Head and Neck Surgery and. Special thanks to Dr. Jiahao Li in the department of Neurology at the First Affiliated Hospital of Xi'an Jiao Tong University for his methodology guidance and support. We would like to thank Editage (www.editage.cn) for English language editing.

## Author contributions

The data was analyzed by H.M.K and S.D.H., who also produced the sections on techniques and results and generated the figures and tables. The research idea and data analysis procedures were contributed to by Y.Y.C, Z.H.L, and Y.Y.X; the data acquisition was handled by W.Q.Z, S.H.Q, and J.R; J.J. designed the study and read the text. The final paper was authorized and contributed to by all authors.

## Funding

This study was supported by the National Natural Science Foundation of China (Grant No. 81960313), the National Key Research and Development Program of China(2022YFC3602202), Jiangxi Provincial Key Laboratory for Precision Pathology and Intelligent Diagnosis, Department of Radiology, The First Affiliated Hospital, Jiangxi Medical College, Nanchang University and the Clinical Research Center For Medical Imaging In Jiangxi Province (No. 20223BCG74001).

## Declarations

## Competing interests

The authors declare no competing interests.

## Additional information

**Supplementary Information** The online version contains supplementary material available at <https://doi.org/10.1038/s41598-025-95925-8>.

**Correspondence** and requests for materials should be addressed to J.J.

**Reprints and permissions information** is available at [www.nature.com/reprints](http://www.nature.com/reprints).

**Publisher's note** Springer Nature remains neutral with regard to jurisdictional claims in published maps and institutional affiliations.

**Open Access** This article is licensed under a Creative Commons Attribution-NonCommercial-NoDerivatives 4.0 International License, which permits any non-commercial use, sharing, distribution and reproduction in any medium or format, as long as you give appropriate credit to the original author(s) and the source, provide a link to the Creative Commons licence, and indicate if you modified the licensed material. You do not have permission under this licence to share adapted material derived from this article or parts of it. The images or other third party material in this article are included in the article's Creative Commons licence, unless indicated otherwise in a credit line to the material. If material is not included in the article's Creative Commons licence and your intended use is not permitted by statutory regulation or exceeds the permitted use, you will need to obtain permission directly from the copyright holder. To view a copy of this licence, visit <http://creativecommons.org/licenses/by-nc-nd/4.0/>.